Is Selective Late Na+ Current Inhibition Different From Class I/B Antiarrhythmic Action? Comparison of The Effects of GS967 to Mexiletine in Canine Ventricular Myocardium

Tamás Hézsô
University of Debrecen
Muhammad Khan
University of Szeged
Csaba Dienes
University of Debrecen
Dénes Kiss
University of Debrecen
János Prorok
University of Szeged
Tamás Arpádffy-Lovas
University of Szeged
Richárd Varga
University of Szeged
Erika Fujii
University of Debrecen
Tanju Mercan
Akdeniz University
Leila Topal
University of Szeged
Kornél Kistamás
University of Debrecen
Norbert Szentandrássy
University of Debrecen
János Almássy
University of Debrecen
Norbert Jost
University of Szeged
János Magyar
University of Debrecen

Tamás Bányász
University of Debrecen
István Baczkó
University of Szeged
András Varró
University of Szeged
Péter Nánási (nanasi.peter@med.unideb.hu)
University of Debrecen
László Virág
University of Szeged
Balázs Horváth
University of Debrecen

Research Article

Keywords: GS967, Mexiletine, Late Na+ current, Ca2+ current, Dog myocytes

Posted Date: January 4th, 2021

DOI: https://doi.org/10.21203/rs.3.rs-134972/v1

Abstract

Enhancement of the late Na^+ current (I_{NaL}) increases arrhythmia propensity in the heart, while suppression of the current is antiarrhythmic. GS967 is an agent considered as a selective blocker of I_{NaL}. In the present study, effects of GS967 on I_{NaL}, on L-type calcium current (I_{Ca}), and on action potential (AP) morphology were studied in canine ventricular myocytes by using conventional voltage clamp, action potential voltage clamp and sharp microelectrode techniques. These effects of GS967 were compared to tetrodotoxin (TTX) and to the class I/B antiarrhythmic compound mexiletine. 1 μM GS967, 40 μM mexiletine, and 10 μM TTX dissected largely similarly shaped inward currents under action potential voltage clamp conditions. In case of GS967 and mexiletine, the amplitude and integral of this current was significantly smaller when measured in the presence of 1 μM nisoldipine, while no difference was observed in case of TTX. Under conventional voltage clamp conditions, I_{NaL} was significantly decreased by 1 μM GS967 and 40 μM mexiletine (79.0±3.0% and 63.3±2.7% reduction of current integrals, respectively). The integral of I_{Ca} was moderately but significantly diminished by both drugs (reduction of 9.3±3.3% and 14.1±1.5%, respectively). These changes were associated with acceleration of inactivation of I_{Ca}. Drug effects on peak Na^+ current (I_{NaP}) were also assessed by recording AP upstroke in multicellular preparations. Both GS967 and mexiletine showed fast onset and offset kinetics: 110 ms and 289 ms offset time constants, respectively, as determined from V^+_{max} measurements in right ventricular papillary muscles, while the onset kinetics was characterized by 5.3 AP and 2.6 AP, respectively, at 2.5 Hz. Effects on beat-to-beat variability of AP duration (APD) was studied in isolated myocytes. Beat-to-beat variability was significantly decreased by both GS967 and mexiletine (reduction of 42.1±6.5% and 24.6±12.8%, respectively) while their shortening effect on APD was comparable. It is concluded that the electrophysiological effects of GS967 are similar to those of mexiletine, but with somewhat faster offset kinetics of V^+_{max} block. However, since GS967 depressed V^+_{max} and I_{NaL} at the same concentration, the current view that GS967 represents a new class of drugs that selectively block I_{NaL} has to be questiond and it is suggested that GS967 should be classified as a class I/B (or I/B + IV) antiarrhythmic agent.

1. Introduction

Following the large Na^+ current surge associated with the AP upstroke (called I_{NaP}) a smaller but sustained current component (called I_{NaL}) remains active throughout the entire cardiac AP. Enhanced I_{NaL}, due to diseases like heart failure[1–3], hypertrophic cardiomyopathy[4] or LQT3[5], is known to increase arrhythmia propensity in the heart[1, 6–8]. It has been known for a long time that many of the class I antiarrhythmic drugs inhibit I_{NaL} in addition to blocking I_{NaP}[9–14]. This latter effect, however, was considered to enhance proarrhythmic risk and consequently the incidence of sudden cardiac death[15]. As a consequence, development of agents to suppress I_{NaL} selectively was a straightforward strategy in the past decades[2, 16–19]. One of these agents, 6-(4-(trifluoromethoxy)phenyl)-3-(trifluoromethyl)-[l,2,4]triazolo[4,3-a]pyridine, known as GS967 or GS458967, was reported to be a particularly selective

candidate when tested in rabbit ventricular cells[16]. It was also shown that important species-dependent variations existed in the electrophysiologic properties of myocardial preparations[20, 21], and canine ventricular myocytes are considered a reasonably good model for human ventricular cells[22–24]. Furthermore, it was previously shown using the action potential voltage clamp technique that the kinetic properties of I_{NaL} are similar in dogs and humans[20], while differing from those of other mammals including guinea pigs, rabbits and pigs[25–27]. Therefore, we studied the effects of GS967 on I_{NaL} and I_{Ca} and compared them to those of tetrodotoxin (TTX) and the class I antiarrhythmic agent mexiletine in canine ventricular preparations. In this work, based on experimental evidence we challenge the present concept that GS967 exerts a selective I_{NaL} blocking effect, however, it has very similar class I/B antiarrhythmic properties as mexiletine.

2. Methods

2.1. Animals

Adult mongrel dogs of either sex were anesthetized with i.m. injections of 10 mg/kg ketamine hydrochloride (Calypsol, Richter Gedeon, Hungary) + 1 mg/kg xylazine hydrochloride (Sedaxylan, Eurovet Animal Health BV, The Netherlands) according to a protocol approved by the local Animal Care Committees (license N^{o}: 9/2015/DEMáB at University of Debrecen; and I-74-15-2017, I-74-24-2017 at University of Szeged) and by the Department of Animal Health and Food Control of the Ministry of Agriculture and Rural Development (XIII/3330/2017 and XIII/3331/2017). All animal procedures conform to the guidelines from Directive 2010/63/EU of the European Parliament on the protection of animals used for scientific purposes and the Guide for the Care and Use of Laboratory Animals (USA NIH publication NO 85 – 23, revised 1996) The study was carried out in compliance with the ARRIVE guidelines.

2.2. Isolation of cardiomyocytes

Single canine myocytes were obtained by enzymatic dispersion using the segment perfusion technique, as previously described[28]. Briefly, a wedge-shaped section of the ventricular wall supplied by the LAD coronary artery was cannulated, dissected and perfused with a nominally Ca^{2+}-free Joklik solution (Minimum Essential Medium Eagle, Joklik Modification, Sigma-Aldrich Co. St. Louis, MO, USA) for a period of 5 min. After this, the tissue was perfused with Joklik solution supplemented with 1 mg/ml collagenase (Type II, Worthington Biochemical Co., Lakewood, NJ, USA; representing final activity of 224 U/ml) and 0.2% bovine serum albumin (Fraction V., Sigma) containing 50 μM Ca^{2+} for 30 min. Finally, the normal external Ca^{2+} concentration was gradually restored and the cells were stored at 15 ^{o}C in Minimum Essential Medium Eagle until use. The chemicals used in the experiments were obtained from Sigma-Aldrich Co. (St. Louis, MO, USA).

2.3. Electrophysiology

Cells were placed in a plexiglass chamber under an inverted microscope, allowing for continuous superfusion with a modified Tyrode solution by gravity flow at a rate of 1–2 ml/min. The modified Tyrode solution contained (in mM): NaCl 121, KCl 4, $CaCl_2$ 1.3, $MgCl_2$ 1, HEPES 10, $NaHCO_3$ 25, glucose 10 at pH = 7.35, which was supplemented according to the actual experimental design. The osmolarity of this solution was 300 ± 3 mOsm, measured with a vapor pressure osmometer. In all experiments, the bath temperature was set to 37 ºC using a temperature controller (Cell MicroControls, Norfolk, VA, USA). Electrical signals were amplified and recorded (MultiClamp 700A or 700B, Molecular Devices, Sunnyvale, CA, USA) under the control of a pClamp 10 software (Molecular Devices) following analogue-digital conversion (Digidata 1440A or 1332, Molecular Devices). Electrodes, having tip resistances of 2–3 MΩ when filled with pipette solution, were manufactured from borosilicate glass. Transmembrane currents were recorded in whole-cell voltage clamp configuration. The series resistance was typically 4–8 MΩ, and the measurement was discarded if it changed substantially during the experiment.

2.3.1. Action potential voltage clamp

Action potential voltage clamp experiments were performed according to the methods described[29, 30]. A previously recorded midmyocardial canine ventricular AP was applied as command signal and the current traces were recorded continuously in modified Tyrode solution before and after 5 min superfusion with the Na^+ channel inhibitor applied. The drug-sensitive current was obtained by subtracting the post-drug trace from the reference pre-drug trace. These measurements were performed either in the presence or absence of 1 μM nisoldipine added to the Tyrode solution. The pipette solution contained (in mM): K-aspartate 120, KCl 30, MgATP 3, HEPES 10, Na_2-phosphocreatine 3, EGTA 0.01, cAMP 0.002, KOH 10 at pH = 7.3 with an osmolarity of 285 mOsm. The amplitude of the dissected current (I_{NaL} in the presence of nisoldipine) was evaluated at half-duration of the command AP. When determining the current integral, the initial 20 ms after the AP upstroke was excluded from evaluation in order to eliminate the contribution of I_{NaP}. In each experiment 20 consecutive current traces were averaged and analyzed in order to reduce the noise and the trace-to-trace fluctuations of action potential configuration. Ion currents were normalized to cell capacitance, determined in each cell by applying hyperpolarizations from + 10 to − 10 mV for 15 ms.

2.3.2. Conventional voltage clamp

Conventional voltage clamp experiments, using rectangular command pulses, were performed to study the effects of GS967 and mexiletine on I_{NaL} and I_{Ca} at stable test potentials.

When measuring I_{NaL} the external solution was a HEPES-buffered Tyrode solution containing (in mM): NaCl 144, NaH_2PO_4 0.4, KCl 4.0, $CaCl_2$ 1.8, $MgSO_4$ 0.53, glucose 5.5 and HEPES 5.0, at pH = 7.4) supplemented with 1 μM nisoldipine, 0.5 μM HMR-1556 and 0.1 μM dofetilide in order to block Ca^{2+} and K^+ currents. The composition of the pipette solution was (in mM): CsCl 125, TEACl 20, MgATP 5, EGTA 10, HEPES 10, at a pH = 7.2). Test pulses were clamped to − 20 mV for 2 s from the holding potential of -120 mV before and after application of GS967 or mexiletine, while the total amount of I_{NaL} was

determined by pharmacological subtraction performed by a final superfusion with 20 μM TTX. The amplitude of I_{NaL} was evaluated at 50 ms after beginning the pulse. For determination of current integral the initial 20 ms was excluded from evaluation in order to minimize the contribution of I_{NaP}.

In the case of I_{Ca} measurements the bath solution was modified Tyrode solution supplemented with 3 mM 4-aminopyridine to suppress K^+ currents. The pipette solution contained (in mM): K-aspartate 120, KCl 30, MgATP 3, HEPES 10, Na_2-phosphocreatine 3, EGTA 0.01, cAMP 0.002, KOH 10 at pH = 7.3. Test pulses to + 5 mV, lasting for 200 ms, arose from the holding potential of -80 mV, while a prepulse to −40 mV for 15 ms was interposed between the holding potential and the test pulse to inactivate Na^+ channels. In this case the current integral contained the total amount of current carried by I_{Ca} from the beginning to the end of the test pulse.

2.3.3. Recording of APs from multicellular preparations

Multicellular preparations (right ventricular papillary muscles) were selected to prevent the limitations of isolated myocyte studies, like the absence of intercellular clefts or potential damage to channel proteins, allowing better representation of *in vivo* conditions.

The experiments were performed as it was previously described[31]. Briefly, transmembrane potentials were recorded using 3 M KCl filled sharp glass microelectrodes having tip resistance between 10 and 20 MΩ. These electrodes were connected to the input of a high impedance electrometer (MDE GmbH, Heidelberg, Germany). Preparations were paced by a pair of platinum electrodes using 1 ms wide rectangular current pulses with twice the threshold amplitude at 37 °C. The pacing cycle length was set to 1 s for at least 60 min allowing the preparations to equilibrate before starting the experiment.

Following equilibration at 1 s cycle length, the cycle length was sequentially varied between 0.3 and 5 s. At each cycle length the 25th AP was recorded, and the cycle length was then changed. Under these conditions a quasi steady-state rate-dependence could rapidly be obtained. APs were digitized at 100 kHz using an ADA 3300 data acquisition board (Real Time Devices Inc., State Collage, PA, USA) and stored for later analysis. After taking control records at each cycle length the preparations were superfused with either GS967 or mexiletine for 20 min and then the protocol was repeated. Efforts were made to maintain the same impalement throughout each experiment. If, however, an impalement became dislodged, adjustment was attempted, but when the parameters of the re-established impalement deviated by more than 5% from the previous record, the experiment was discarded.

Restitution kinetics of the maximum rate of depolarization (V^+_{max}) is considered as the indicator of offset time constant. To determine the restitution time constant for V^+_{max} the preparations were paced using a train of 20 basic stimuli delivered at a basic cycle length of 1 s. Each train was followed by a single extra stimulus applied with successively longer coupling intervals. The train of basic stimuli was reinitiated following the delivery of the extra stimulus. In this way, each 20th basic AP was followed by a single extra AP occurring at gradually increasing diastolic intervals. The diastolic interval was defined as

the time from APD_{90} of the last basic member of the train to the upstroke of the extra AP. Recovery curves were generated by plotting the V^+_{max} of each extra AP as a function of the respective diastolic interval and data were fitted to a single exponential function.

Onset kinetics of drug action on V^+_{max} were determined by stimulating the preparation at a cycle length of 0.4 s following a few min period of rest and the initial 40 APs were recorded and data were plotted against the number of the analyzed AP within the train. The rate of development of block was obtained by monoexponential fitting of the V^+_{max} values.

2.3.4. Determination of beat-to-beat variability of APD in isolated myocytes

Since beat-to-beat variability of APD is relatively small in multicellular preparations due to the balancing effect of the neighboring cells, these experiments were performed in isolated myocytes. Series of 50 consecutive action potentials were analyzed to estimate the beat-to-beat variability of APD, defined as short term variability (SV), according to the following formula:

$$SV = \Sigma \left(\left| APD_{i+1} \; \textit{minus} \; APD_i \right| \right) / \left[n_{beats} * \sqrt{2} \right]$$

where SV is short term variability, APD_n and APD_{n+1} indicate the durations of the i^{th} and $i + 1^{th}$ APs, respectively, at 90% level of repolarization and n_{beats} denotes the number of consecutive beats analyzed[32]. Changes in SV were presented as Poincaré plots where 50 consecutive APD values are plotted, each against the duration of the previous AP.

2.4. Statistics

Results are expressed as mean ± SEM values, n denotes the number of myocytes or multicellular preparations studied. Statistical significance of differences was evaluated using one-way ANOVA followed by Student's t-test for paired or unpaired data as pertinent. Differences were considered significant when p was less than 0.05.

3. Results

3.1. Effects of GS967, mexiletine and TTX under action potential voltage clamp conditions

Under action potential voltage clamp conditions, 10 μM TTX, 1 μM GS967 and 40 μM mexiletine dissected similarly shaped inward current profiles dominated by I_{NaL} (Fig. 1). These concentrations were chosen because the densities, measured at half-duration of the AP (50% of APD_{90}), and integrals of the dissected currents were largely comparable in size. TTX was applied as a reference, since 10 μM TTX was shown to suppress more than 80% of I_{NaL} in canine ventricular cells[20]. Importantly, in all action

potential voltage clamp experiments performed with mexiletine, the bath solution contained 1 μM E4031 and 100 μM chromanol 293B in order to eliminate any interference from K^+ currents[33]. Since I_{Ca} was not suppressed in these experiments, the measurements were repeated in the presence of 1 μM nisoldipine (NISO) and the results were compared to those obtained without nisoldipine (NO NISO) as presented in Fig. 2. In the case of GS967 and mexiletine, the half-duration current densities were significantly smaller in the presence (− 0.27 ± 0.02 and − 0.25 ± 0.02 A/F) than in the absence (− 0.42 ± 0.03 and − 0.45 ± 0.04 A/F) of nisoldipine. Similar differences were found when comparing the current integrals: −48 ± 4 and − 43 ± 4 mC/F in the absence, while − 68 ± 5 and − 74 ± 10 mC/F in the presence of nisoldipine, respectively. Importantly, there was no significant difference between the NISO and NO NISO data in the case of TTX. These results suggest that both GS967 and mexiletine inhibit I_{Ca} in addition to I_{NaL} blockade.

3.2. Effects of GS967 and mexiletine on I_{NaL} under conventional voltage clamp conditions

The effects of 1 μM GS967 and 40 μM mexiletine on I_{NaL} were also studied under conventional voltage clamp conditions by applying 2 s duration depolarizations to − 20 mV from the holding potential of − 120 mV (Fig. 3). 1 μM GS967 significantly reduced the density of I_{NaL}, measured at 50 ms after the beginning of the pulse (from − 0.313 ± 0.05 to − 0.062 ± 0.01 A/F, corresponding to an 80.4 ± 2.2% reduction on the average of 6 myocytes). For comparison, this parameter was also significantly decreased by 40 μM mexiletine (from − 0.385 ± 0.036 to − 0.156 ± 0.014 A/F, reduction of 59.1 ± 1.8%, n = 12). Similar results were obtained when comparing the current integrals, i.e. the charge carried by the current with the exclusion of the initial 20 ms. As determined from the same experiments, the current integrals were significantly decreased from − 69.1 ± 7.9 to − 15.4 ± 3.9 mC/F (79.0 ± 3.1% inhibition) by 1 μM GS967 and from − 76.4 ± 7.6 to − 26.7 ± 2.6 mC/F (63.3 ± 2.7% reduction) by 40 μM mexiletine.

3.3. Effects of GS967 and mexiletine on I_{Ca} under conventional voltage clamp conditions

Since action potential clamp experiments suggested some inhibition of I_{Ca} by both GS967 and mexiletine, this was clarified using conventional voltage clamp, as shown in Fig. 4. Although peak I_{Ca} was not altered significantly by 1 μM GS967 (− 4.92 ± 0.16 and − 4.76 ± 0.04 A/F), the current density, measured at 50 ms after the beginning of the pulse, was significantly reduced (from − 0.66 ± 0.05 to − 0.62 ± 0.05 A/F). Accordingly, the current integral (measured from the beginning to the end of pulse) was also significantly decreased by GS967 in the 7 myocytes studied (from − 111.9 ± 5.0 to − 100.7 ± 3.1 mC/F, reduction of 9.3 ± 3.3%). The suppressive effect of 40 μM mexiletine on I_{Ca} was somewhat more pronounced. It was significant for the reduction of peak current (from − 4.9 ± 0.4 to − 4.4 ± 0.4 A/F), and for the current measured at 50 ms (from − 0.86 ± 0.08 to − 0.70 ± 0.07 A/F), as well as the current integral (from − 114 ± 11 to − 98 ± 9 mC/F, corresponding to 14.1 ± 1.5% reduction on average of 5 experiments). Both drugs

accelerated the decay time of I_{Ca}, determined between 90% and 10% of current amplitudes, significantly: from 48.8 ± 2.5 to 44.2 ± 2.9 ms by GS967, and from 50.8 ± 5.4 to 44.9 ± 5.0 ms by mexiletine. This acceleration of current decay may account for the decreased current integrals.

3.4. Effects of GS967 and mexiletine on action potential upstroke

After determining the effects on I_{NaL} and I_{Ca}, the actions of GS967 and mexiletine on I_{NaP} were studied and compared. Since direct measurement of cardiac I_{NaP} is difficult at 37 ^{o}C, the maximum velocity of depolarization during the action potential upstroke (V^{+}_{max}) was used as an approximate, although not linear, measure of I_{NaP}[34–36]. Due to the more physiological situation (e.g higher stability) in multicellular cardiac preparations, these experiments were performed in right ventricular papillary muscles using sharp microelectrodes. As demonstrated in Fig. 5.A,B, 40 μM mexiletine significantly reduced V^{+}_{max} in the entire frequency range applied under steady-state conditions, while this effect of GS967 was significant only at the shortest cycle lengths of 0.3 and 0.4 s. This difference can well be explained by the faster offset kinetics of GS967 (Fig. 5.C,D). The time constant of recovery of V^{+}_{max}, determined following a constant 1 Hz stimulation was 110 ms for GS967, while almost three times longer, 289 ms for mexiletine. The onset kinetics of V^{+}_{max} block was studied by application of a constant stimulation rate at 2.5 Hz and the initial 40 APs were recorded. The onset rate constant was 5.3 AP for 1 μM GS967 and 2.6 AP for 40 μM mexiletine (Fig. 5.E,F).

3.5. Effects of GS967 and mexiletine on APD

Although APD in right ventricular trabeculae was shortened by both GS967 and mexiletine in a reverse rate-dependent manner, this effect was statistically significant only at the longest constant cycle lengths above 1.5 s (Fig. 6).

3.6. Effects of GS967 and mexiletine on beat-to-beat variability of APD

Elevated beat-to-beat QT interval variability is a good predictor of ventricular arrhythmia in a wide variety of patients, while at a single cell level it translates into beat-to-beat variability of APD (also called short term variability, SV) - both parameters are considered as indicators of proarrhythmic risk[37–40]. In contrast to multicellular preparations, where the neighboring cells may effectively balance the individual differences in APD, SV is more pronounced in single cells, therefore the effects of GS967 and mexiletine were studied on SV in isolated ventricular cells, paced at a constant cycle length of 1 s. Under these conditions SV was significantly decreased by 1 μM GS967 and 40 μM mexiletine (reduction of 1.01 ± 0.19 and 0.63 ± 0.02 ms, respectively, corresponding to 42.1 ± 6.5% and 24.6 ± 12.8% decrease), while APD was moderately shortened by 32.5 ± 6.9 and 41.4 ± 4.1 ms, respectively, (all $p < 0.05$ and $n = 8$). All these

effects were largely reversible upon washout (Fig. 7). Since APD itself is also known to affect the magnitude of SV, the term of relative SV (RSV) was introduced[41, 42]. Accordingly, RSV = dSV / dAPD, i.e. the change in SV is normalized to that of APD. The value of RSV was significantly higher for GS967 than mexiletine (0.039 ± 0.007 *versus* 0.015 ± 0.007) predicting a better antiarrhythmic effectivity of GS967 than mexiletine.

4. Discussion

We studied and compared the effects of GS967 (1 μM) to those of the class I/B antiarrhythmic drug mexiletine (40 μM) on I_{Ca}, I_{NaL} and I_{NaP} in canine ventricular myocardium by combining the conventional microelectrode, voltage clamp and action potential voltage clamp techniques. It was found that GS967, which is generally considered as a selective blocker of I_{NaL}[16], inhibits I_{Ca} and I_{NaP} as well, similarly to the class I/B antiarrhythmic drug mexiletine[33] but with higher potency. The I_{Ca} blocking effects were more prominent under action potential voltage clamp than under conventional voltage clamp conditions in the case of both drugs (compare Figs. 2 and 4). The reason for this difference is unknown at present, however, it highlights the advantage of the action potential voltage clamp technique in cardiac cellular electrophysiology and pharmacology.

Based on the hypothetically selective I_{NaL} blocker nature of GS967, the drug was previously mentioned as a novel class VI antiarrhythmic agent[43]. However, without questioning the theoretical possibility of the concept for selective I_{NaL} inhibition, an alternative approach should also be considered, since the concept whether I_{NaL} can be blocked selectively is an interesting and still unresolved issue. There is evidence that sodium current in cardiac tissues may also be conducted by sodium channels other than the cardiac specific $Na_v1.5$ channels, such as $Na_v1.8$[44]. Also, relatively high mRNA expression levels of $Na_v2.1$ were reported in human ventricle[45] but proper functional evidence for its role is still lacking. If these channels play a role in I_{NaL} but not in I_{NaP}, pharmacological inhibition of these channels may result in selective I_{NaL} blockade. However, GS967 has not been shown to inhibit these latter types of sodium channels but it was reported to inhibit cardiac type $Na_v1.5$ channels[9, 10]. $Na_v1.5$ channels have complex and multiple open and closed states[46] with different drug binding properties governing active, inactive and resting channel states. Accordingly, drugs interacting with the binding sites of the channels depending on their actual open or closed channel states may produce variable effects on I_{NaP} and I_{NaL}. For example, when a drug binds rapidly and with high affinity to open and inactivated channel states, and it dissociates rapidly from closed resting channel states, it would not inhibit I_{NaP} but I_{NaL}. This would be due to complete drug dissociation from its binding site in the resting closed states unless frequency was very high or at least the cycle length would be shorter than its dissociation from the channel. Consequently, whether a drug inhibits I_{NaP} or I_{NaL} selectively or both of them, largely depends on the stimulation protocol but not on existing specific I_{NaP} or I_{NaL} binding sites. Present results and other recently published data[9, 10] are consistent with this suggestion and do not support a mechanism which is based on specific I_{NaL} inhibition that is distinctly different from class I/B antiarrhythmic actions described for drugs such as

mexiletine[14, 46], lidocaine[9, 10, 14], amiodarone[11] and ranolazine[47]. This approach is also in line with the reported high (38-fold) selectivity of ranolazine on I_{NaL} over I_{NaP}[2], which is intermediate (13-fold) for amiodarone[3] and much lower (only 3-fold) for flecainide[48].

In our experiments, both GS967 and mexiletine significantly depressed V^+_{max} at high stimulation rates. It was previously established that changes of V^+_{max} and I_{NaP} are not linear and a relatively modest decrease of V^+_{max} can represent robust depression of I_{NaP}[35, 36]. Accordingly, the 20–30% reduction of V^+_{max} measured in the present study in papillary muscle preparations (at pacing cycle lengths of 0.3–0.4 s) following GS967 and mexiletine application can represent a similar degree of I_{NaP} depression as the measured 60–80% reduction of I_{NaL} obtained in ventricular myocytes. Therefore, in theory, neither GS967 nor mexiletine can be considered as “selective” I_{NaL} inhibitors. However, when therapy is concerned – assuming that decreased I_{NaP} is proarrhythmic, while reduced I_{NaL} is antiarrhythmic – GS967, which has about 3-fold faster offset kinetics, can be more beneficial than mexiletine since I_{NaP} would be affected in a lesser extent than I_{NaL} by GS967 at normal or moderately enhanced heart rates.

On the basis of present and other results it is clear that GS967 affects I_{NaP} in a strongly rate- and moderately species-dependent fashion. Similarly to our results, V^+_{max} was reduced by 0.3 μM GS967 in murine myocytes[49], while the same concentration of the drug failed to modify V^+_{max} in canine Purkinje strands[50]. On the other hand, GS967 shortened APD in a variety of preparations, including rat[51, 52], murine[49], rabbit[16, 53] and human[54] ventricular cells within a wide concentration range (0.1-1 μM) – similarly to the present observations in isolated canine ventricular cells. In our multicellular preparations, however, a significant APD shortening effect appeared only at cycle lengths longer than 1.5 s. This can be explained by the well-known higher drug-sensitivity of single cells comparing to multicellular preparations. The moderate reduction of I_{Ca} by GS967, in addition to its decrease of I_{NaL}, is not expected to impair A-V conduction. However, this effect can contribute to the GS967-induced shortening of the elongated APD, reduction of the enhanced dispersion and short term variability of repolarization, changes often preceding torsade de pointes arrhythmias[38–40].

Taken together the present results and the literature, it is likely that a compound having kinetic properties similar to GS967 would be a very promising new antiarrhythmic agent, since several *in vitro*[16–19, 49–54] and *in vivo*[51, 55] studies support the potent antiarrhythmic activity of GS967. Its kinetic properties are better than those of mexiletine, as shown in this study, and also than those of ranolazine[9], agents known to suppress I_{NaL}. Although GS967 had high brain penetration and caused a profound use-dependent block on all sodium channel isoforms studied, making the compound prone for possible central nervous system side effects[56], a new agent exhibiting the same kinetic properties of GS967 without CNS side effects would represent a promising candidate for future development.

In summary, GS967 – similarly to mexiletine – inhibited both the peak and late components of Na^+ current, suppressed Ca^{2+} current and decreased beat-to-beat variability of APD. Based on its kinetic properties, GS967 should be classified as a new potent class I/B (or probably I/B + IV) antiarrhythmic agent. The results of the present study also suggest that investigations of "selective" I_{NaL} inhibitors should be carried out through a wide range of stimulation rates since the effect of drugs like GS967 or mexiletine, that possess fast offset kinetics of I_{NaP} inhibition, can be misinterpreted.

Declarations

Acknowledgements

This work was funded by the National Research Development and Innovation Office (NKFIH-PD120794 and NKFIH-FK128116 to B.H., NKFIH-K119992 to A.V. and NKFIH K 128851 to I.B.) and by the Hungarian Academy of Sciences (János Bolyai Research Scholarship to B.H.). Further support was obtained from the Thematic Excellence Programme of the Ministry for Innovation and Technology in Hungary (ED_18-1-2019-0028), within the framework of the Space Sciences thematic programme of the University of Debrecen, and from the GINOP-2.3.2.-15-2016-00040 and GINOP-2.3.2.-15-2016-00048, projects, co-financed by the European Union and the European Regional Development Fund. The work was also supported by the Ministry of Human Capacities Hungary (EFOP-3.6.2-16-2017-00006, EFOP 3.6.2 16 2017-00006, EFOP 3.6.3-VEKOP-16-2017-00009, 20391-3/2018/FEKUSTRAT, ÚNKP-20-2 and ÚNKP-20-3 projects).

Author contribution statement

Preparation of the manuscript: PPN, AV, BH.

Design of experimental protocols: TB, JM, IB.

Action potential voltage clamp experiments: TH, CsD, DK.

Conventional voltage clamp experiments: MNK, JP, NSz..

Action potential recording from multicellular preparations: TáL, RV, EF, LT.

Action potential recording from isolated canine myocytes preparations: KK, TM.

Statistical analysis: NJ, JA, LV.

Conflict of interest: none declared.

References

1. Valdivia, C.R. et al. Increased late sodium current in myocytes from a canine heart failure model and from failing human heart. *J. Mol. Cell. Cardiol.***38**, 475–483 (2005).
2. Undrovinas, A.I., Belardinelli, L., Undrovinas, N.A., Sabbah. H.N. Ranolazine improves abnormal repolarization and contraction in left ventricular myocytes of dogs with heart failure by inhibiting late sodium current. *J. Cardiovasc. Electrophysiol.***17 Suppl 1,** S169-S177 (2006).
3. Maltsev, V.A., Sabbah, H,N., Undrovinas, A.I. Late sodium current is a novel target for amiodarone: studies in failing human myocardium. *J. Mol. Cell. Cardiol.***33**, 923–932 (2001).
4. Coppini, R., Santini, L., Olivotto, I., Ackerman, M.J., Cerbai, E. Abnormalities in sodium current and calcium homoeostasis as drivers of arrhythmogenesis in hypertrophic cardiomyopathy. *Cardiovasc. Res.***116**, 1585-1599 (2020).
5. Hu, R.M. et al. Mexiletine rescues a mixed biophysical phenotype of the cardiac sodium channel arising from the SCN5A mutation, N406K, found in LQT3 patients. *Channels (Austin)***12**, 176-186 (2018).
6. Antzelevitch, C., Belardinelli, L. The role of sodium channel current in modulating transmural dispersion of repolarization and arrhythmogenesis. *J. Cardiovasc. Electrophysiol.***17 Suppl 1**, S79-S85 (2006).
7. Maltsev, V.A., Silverman, N., Sabbah, H.N., Undrovinas, A.I. Chronic heart failure slows late sodium current in human and canine ventricular myocytes: Implications for repolarization variability. *Eur. J. Heart. Fail.***9,** 219–227 (2007).
8. Shyrock, J.C., Song, Y., Rajamani, S., Antzelecitch, C., Belardinelli, L. The antiarrhythmogenic consequences of increasing late I_{Na} in the cardiomyocyte. *Cardiovasc. Res.***99,** 600-611 (2013).
9. Potet, F., Vanoye, C.G., George, A.L. Jr. Use-dependent block of human cardiac sodium channels by GS967. *Mol. Pharmacol.***90**, 52–60 (2016).
10. Potet, F., Egecioglu, D.E., Burridge, P.W., George, A.L. Jr. GS-967 and eleclazine block sodium channels in human induced pluripotent stem cell-derived cardiomyocytes. *Mol. Pharmacol.***98,** 540-547 (2020).
11. Ghovanloo, M.R., Abdelsayed, M., Ruben, P.C. Effects of amiodarone and N-desethylamiodarone on cardiac voltage-gated sodium channels. *Front. Pharmacol.***7,** 39 (2016).
12. Salvage, S.C. et al. Multiple targets for flecainide action: implications for cardiac arrhythmogenesis. *Br. J. Pharmacol.***175,** 1260-1278 (2018).
13. Varro, A., Elharrar, V., Surawicz, B. Frequency-dependent effects of several class I antiarrhythmic drugs on Vmax of action potential upstroke in canine cardiac Purkinje fibers. *J. Cardiovasc. Pharmacol.* **7,** 482-492 (1985).
14. Varro, A., Nakaya, Y., Elharrar, V., Surawicz, B. Effect of antiarrhythmic drugs on the cycle length-dependent action potential duration in dog Purkinje and ventricular muscle fibers. *J. Cardiovasc. Pharmacol.***8,** 178-185 (1986).
15. Cardiac Arrhythmia Suppression Trial (CAST) Investigators. Preliminary report: effect of encainide and flecainide on mortality in a randomized trial of arrhythmia suppression after myocardial

infarction. *N. Engl. J. Med.***321,** 406-412 (1989).

16. Belardinelli, L. et al. A novel, potent, and selective inhibitor of cardiac late sodium current suppresses experimental arrhythmias. *J. Pharmacol. Exp. Ther.***344,** 23–32 (2013).
17. Azam, M.A. et al. Effects of late sodium current blockade on ventricular refibrillation in a rabbit model. *Circ. Arrhythm. Electrophysiol.***10,** e004331 (2017).
18. del Canto, I. et al. Effects of the inhibition of late sodium current by GS967 on stretch-induced changes in cardiac electrophysiology. *Cardiovasc. Drugs Ther.* **32,** 413–425 (2018).
19. Bossu, A. et al. Selective late sodium current inhibitor GS-458967 suppresses torsades de pointes by mostly affecting perpetuation but not initiation of the arrhythmia. *Br. J. Pharmacol.* **175,** 2470–2482 (2018).
20. Horváth, B. et al. Late sodium current in human, canine and guinea pig ventricular myocardium. *J. Mol. Cell. Cardiol.***139,**14-23 (2020).
21. Jost, N. et al. Ionic mechanisms limiting cardiac repolarization reserve in humans compared to dogs. *J. Physiol.***591,** 4189-4206 (2013).
22. Szabo, G. et al. Asymmetrical distribution of ion channels in canine and human left-ventricular wall: epicardium versus midmyocardium. *Pflügers. Arch.***450,** 307-316 (2005).
23. Szentadrassy, N. et al. Apico-basal inhomogeneity in distribution of ion channels in canine and human ventricular myocardium. *Cardiovasc. Res.***65,** 851-860 (2005).
24. Jost, N. et al. Contribution of I_{Kr} and I_{K1} to ventricular repolarization in canine and human myocytes: is there any influence of duration? *Basic. Res. Cardiol.***104**, 33-41 (2009).
25. Hegyi, B. et al. β-adrenergic regulation of late Na^+ current during cardiac action potential is mediated by both PKA and CaMKII. *J. Mol. Cell. Cardiol.***123,** 168–179 (2018).
26. Horvath, B. et al. Dynamics of the late Na^+ current during cardiac action potential and its contribution to afterdepolarizations. *J. Mol. Cell. Cardiol.***64,** 59-68 (2013).
27. Hegyi, B. et al. Complex electrophysiological remodeling in postinfarction ischemic heart failure. Proc. Natl. Acad. Sci. U.S.A.**115,** E3036-E3044 (2018).
28. Hegyi, B. et al. Ca^{2+}-activated Cl^- current is antiarrhythmic by reducing both spatial and temporal heterogeneity of cardiac repolarization. *J. Mol. Cell. Cardiol.***109,** 27-37 (2017).
29. Banyasz, T. et al. Endocardial versus epicardial differences in L-type calcium current in canine ventricular myocytes studied by action potential voltage clamp. *Cardiovasc. Res.***58,** 66-75 (2003).
30. Bányász, T. et al. Action potential clamp fingerprints of K^+ currents in canine cardiomyocytes: their role in ventricular repolarization. *Acta. Physiol. Scand.***190,** 189-198 (2007).
31. Virág, L. et al. Analysis of the contribution of I_{to} to repolarization in canine ventricular myocardium. *Br. J. Pharmacol*. **164,** 93-105 (2011).
32. Szentandrássy, N. et al. Contribution of ion currents to beat-to-beat variability of action potential duration in canine ventricular myocytes. *Pflügers Arch.***467,** 1431-1443 (2015).

33. Mitcheson, J.S., Hancox, J.C. Modulation by mexiletine of action potentials, L-type Ca current and delayed rectifier K current recorded from isolated rabbit atrioventricular nodal myocytes. *Pflügers Arch.***434,** 855–858 (1997).
34. Hondeghem, L.M. Validity of V_{max} as a measure of the sodium current in cardiac and nervous tissues. Biophys. J.**23,** 147-152 (1978).
35. Sheets, M.F., Hanck, D.A., Fozzard, H.A. Nonlinear relation between V_{max} and I_{Na} in canine cardiac Purkinje cells. *Circ. Res.***63,** 386-398 (1988).
36. Cohen, C.J., Bean, B.P., Tsien, R.W. Maximal upstroke velocity as an index of available sodium conductance. Comparison of maximal upstroke velocity and voltage clamp measurements of sodium current in rabbit Purkinje fibers. *Circ. Res.* **54,** 636-651 (1984).
37. Abi-Gerges, N., Valentin, J.P., Pollard, C.E. Dog left ventricular midmyocardial myocytes for assessment of drug-induced delayed repolarization: short-term variability and proarrhythmic potential. *Br. J. Pharmacol.***159,** 77-92 (2010).
38. Hinterseer, M. et al. Usefulness of short-term variability of QT intervals as a predictor for electrical remodeling and proarrhythmia in patients with nonischemic heart failure. *Am. J.Cardiol.***106,** 216-220 (2010).
39. Tereshchenko, L.G. et al. Beat-to-beat three-dimensional ECG variability predicts ventricular arrhythmia in ICD recipients. *Heart Rhythm***7,** 1606-1613 (2010).
40. Thomsen, M.B. et al. Increased short-term variability of repolarization predicts *d*-sotalol-induced torsades de pointes in dogs. *Circulation* **110,** 2453-2459 (2004).
41. Szentandrássy, N. et al. Contribution of ion currents to beat-to-beat variability of action potential duration in canine ventricular myocytes. *Pflügers Arch*. **467,** 1431-1443 (2015).
42. Nánási, P.P., Magyar, J., Varró, A., Ördög, B. Beat-to-beat variability of cardiac action potential duration: underlying mechanism and clinical implications. *Canadian. J. Physiol. Pharmacol.* **95,** 1230-1235 (2017).
43. Karagueuzian, H.S., Pezhouman, A., Angelini, M., Olcese, R. Enhanced late Na and Ca currents as effective antiarrhythmic drug targets. *Front. Pharmacol.***8,** Art# 36 (2017).
44. Ahmad, S. et al. The functional consequences of sodium channel Na_v 1.8 in human left ventricular hypertrophy. *ESC Heart. Fail.***6,** 154-163 (2019).
45. Gaborit, N. et al. Regional and tissue specific transcript signatures of ion channel genes in the non-diseased human heart. *J. Physiol.***582,** 675-693 (2007).
46. Mangold, K.E. et al. Mechanisms and models of cardiac sodium channel inactivation. *Channels (Austin)***11,** 517-533 (2017).
47. Szél, T. et al. Class I/B antiarrhythmic property of ranolazine, a novel antianginal agent, in dog and human cardiac preparations. Eur. J. Pharmacol. **662,** 31-39 (2011).
48. Nagatomo, T., January, C.T., Makielski, J.C. Preferential block of late sodium current in the LQT3 DeltaKPQ mutant by the class I(C) antiarrhythmic flecainide. *Mol. Pharmacol.***57,** 101–107 (2000).

49. Portero, V. et al. Anti-arrhythmic potential of the late sodium current inhibitor GS-458967 in murine Scn5a-1798insD1/2 and human SCN5A-1795insD1/2 iPSC-derived cardiomyocytes. *Cardiovasc. Res.***113,** 829–838 (2017).
50. Sicouri, S., Belardinelli, L., Antzelevitch, C. Antiarrhythmic effects of the highly selective late sodium channel current blocker GS-458967. *Heart Rhythm***10,** 1036–1043 (2013).
51. Chi, L. et al. Inhibition of late Na current, a novel target to improve diastolic function and electrical abnormalities in Dahl salt-sensitive rats. *Am. J. Physiol. Heart. Circ. Physiol.***310,** H1313–H1320 (2016).
52. Pezhouman, A. et al. Selective inhibition of late sodium current suppresses ventricular tachycardia and fibrillation in intact rat hearts. *Heart Rhythm***11,** 492–501 (2014).
53. El-Bizri, N., Li, C.H., Liu, G.-X., Rajamani, S., Belardinelli, L. Selective inhibition of physiological late Na current stabilizes ventricular repolarization. *Am. J. Physiol. Heart. Circ. Physiol.***314,** H236–H245 (2018).
54. Ferrantini, C. et al. Late sodium current inhibitors to treat exercise-induced obstruction in hypertrophic cardiomyopathy: an in vitro study in human myocardium. *Br. J. Pharmacol*. **175,** 2635–2652 (2018).
55. Bonatti, R. et al. Selective late sodium current blockade with GS-458967 markedly reduces ischemia-induced atrial and ventricular repolarization alternans and ECG heterogeneity. *Heart Rhythm***11,** 827–1835 (2014).
56. Koltun, D.O. et al. Discovery of triazolopyridine GS-458967, a late sodium current inhibitor (Late I_{Na}i) of the cardiac NaV 1.5 channel with improved efficacy and potency relative to ranolazine. *Bioorg. Med. Chem. Lett.* **26,** 3202–3206 (2016).

Figures

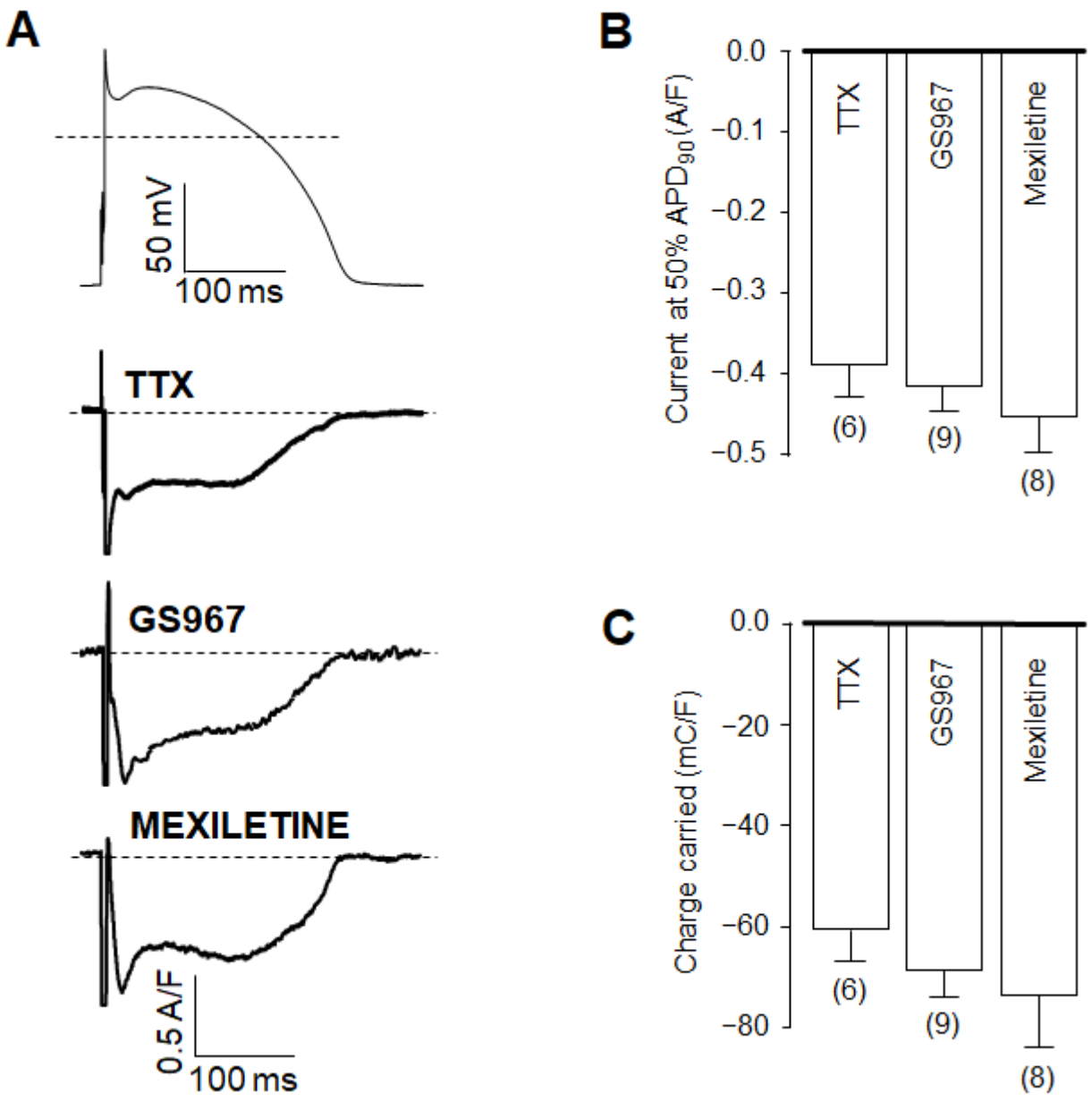

Figure 1

Effects of TTX, GS967 and mexiletine in isolated canine ventricular myocytes under action potential voltage clamp conditions. A: representative membrane current records dissected by 10 μM TTX, 1 μM GS967 and 40 μM mexiletine, respectively. The command AP is shown above the current traces. Dashed lines indicate zero voltage and current levels. B: Current densities measured at half-duration of the command AP. C: Current integrals from which the initial 20 ms period was excluded. Columns and bars denote mean ± SEM values, numbers in parentheses indicate the number of myocytes studied.

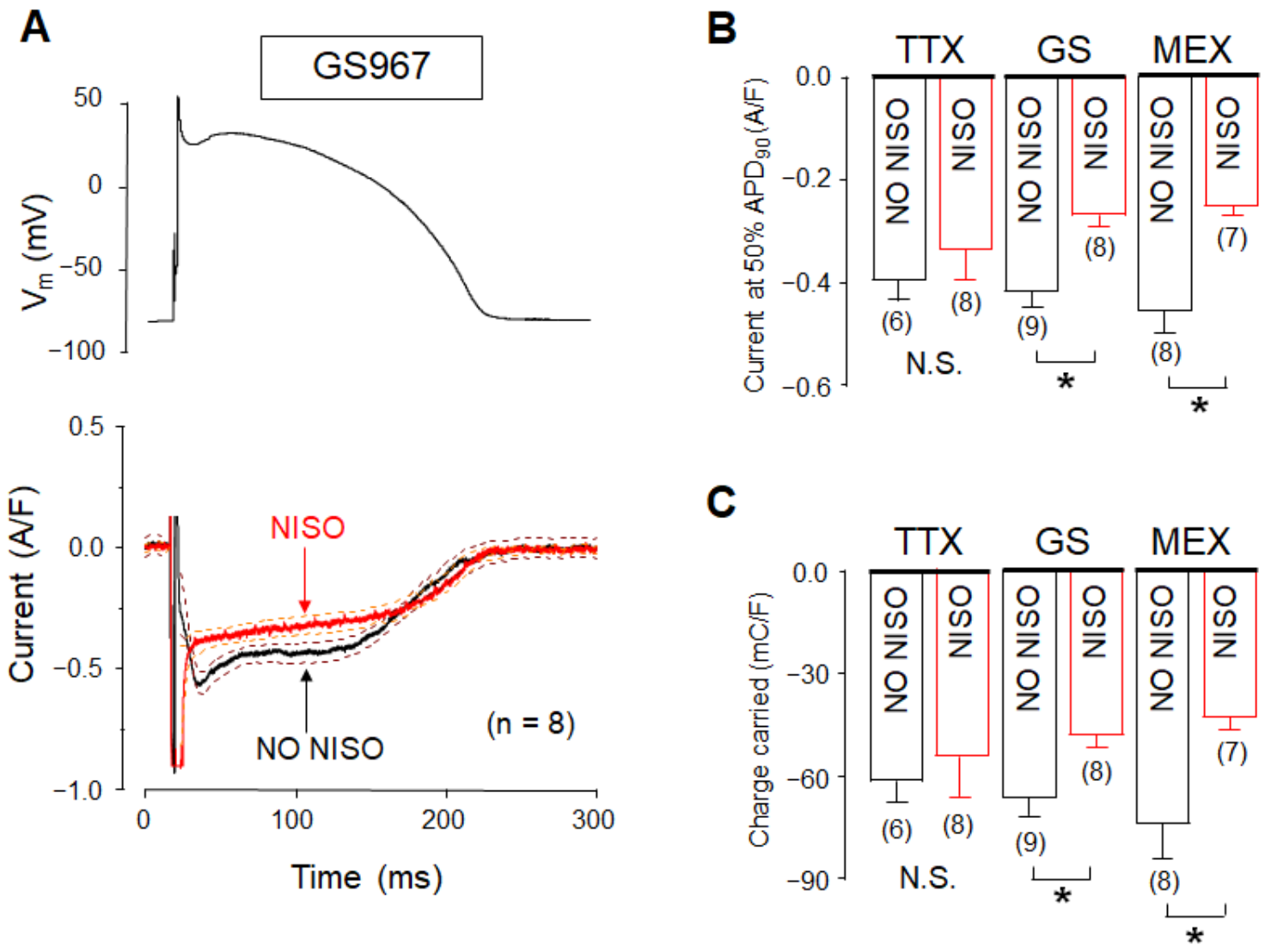

Figure 2

Effects of TTX, GS967 and mexiletine under action potential voltage clamp conditions in the absence and presence of nisoldipine. A: The command AP (above) and GS967-sensitive current profiles (below) obtained in the presence (NISO) and absence (NO NISO) of 1 μM nisoldipine. The records were obtained by averaging data obtained from 8 myocytes. Dashed lines denote SEM values. B,C: Average current densities, measured at half-duration of the command AP (B), and current integrals (C) obtained in the absence and presence of nisoldipine with TTX, GS967 and mexiletine. Columns and bars are mean ± SEM, numbers in parentheses indicate the number of myocytes studied, asterisks denote significant differences between the NISO and NO NISO groups.

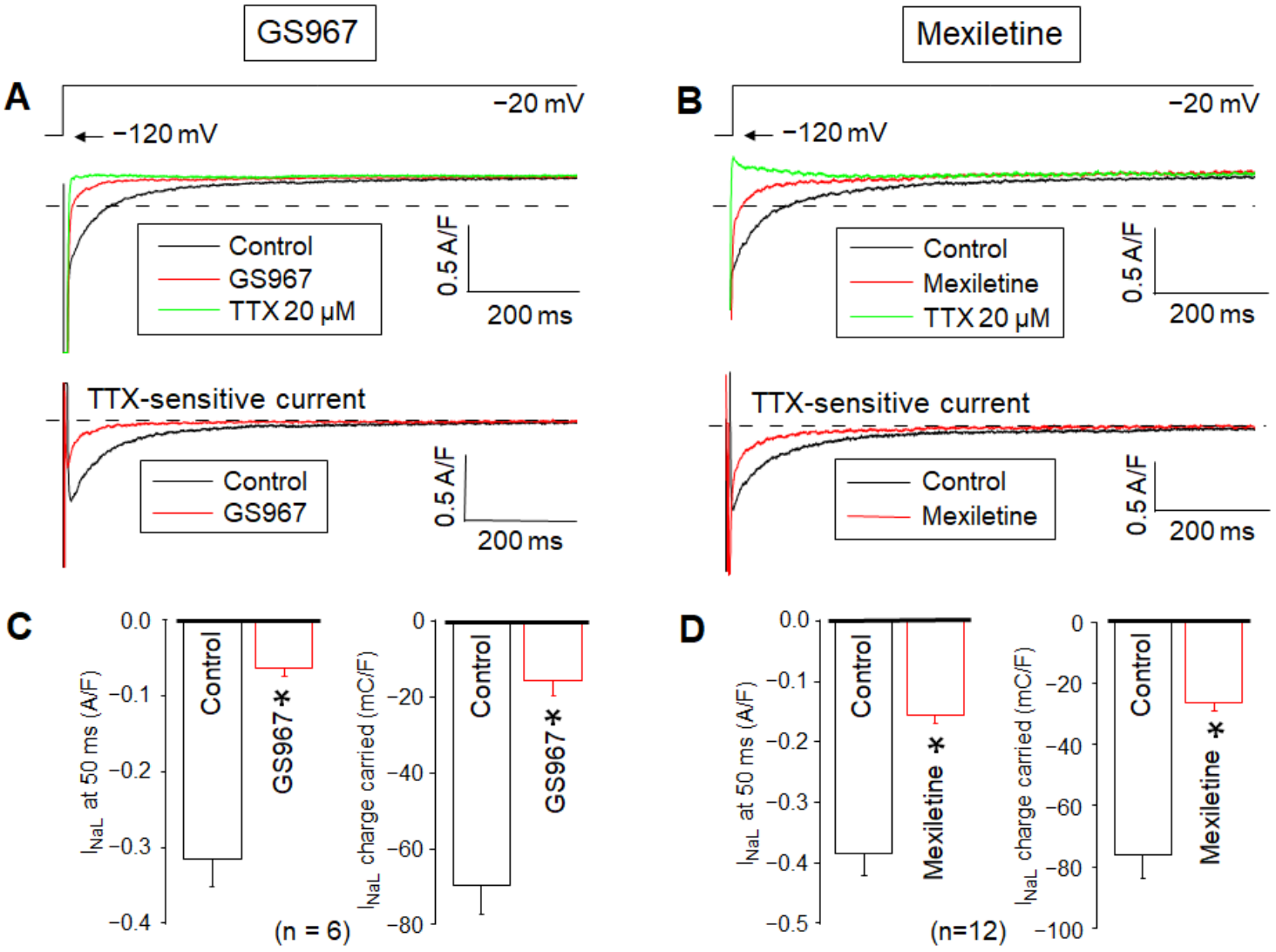

Figure 3

Effects of 1 µM GS967 (A,C) and 40 µM mexiletine (B,D) on INaL under conventional voltage clamp conditions using test pulses of 2 s duration clamped to −20 mV from the holding potential of −120 mV. At the end of each experiment the cells were superfused with 20 µM TTX to dissect the remaining INaL. Dashed lines indicate zero current level. A,B: Representative superimposed analogue records. C,D: Average INaL densities (measured at 50 ms) and integrals (measured from 20 ms to 2 s). Columns and bars are mean ± SEM, numbers in parentheses indicate the number of myocytes studied, asterisks denote significant differences between the pre-drug control and the GS967- or mexiletine-treated data.

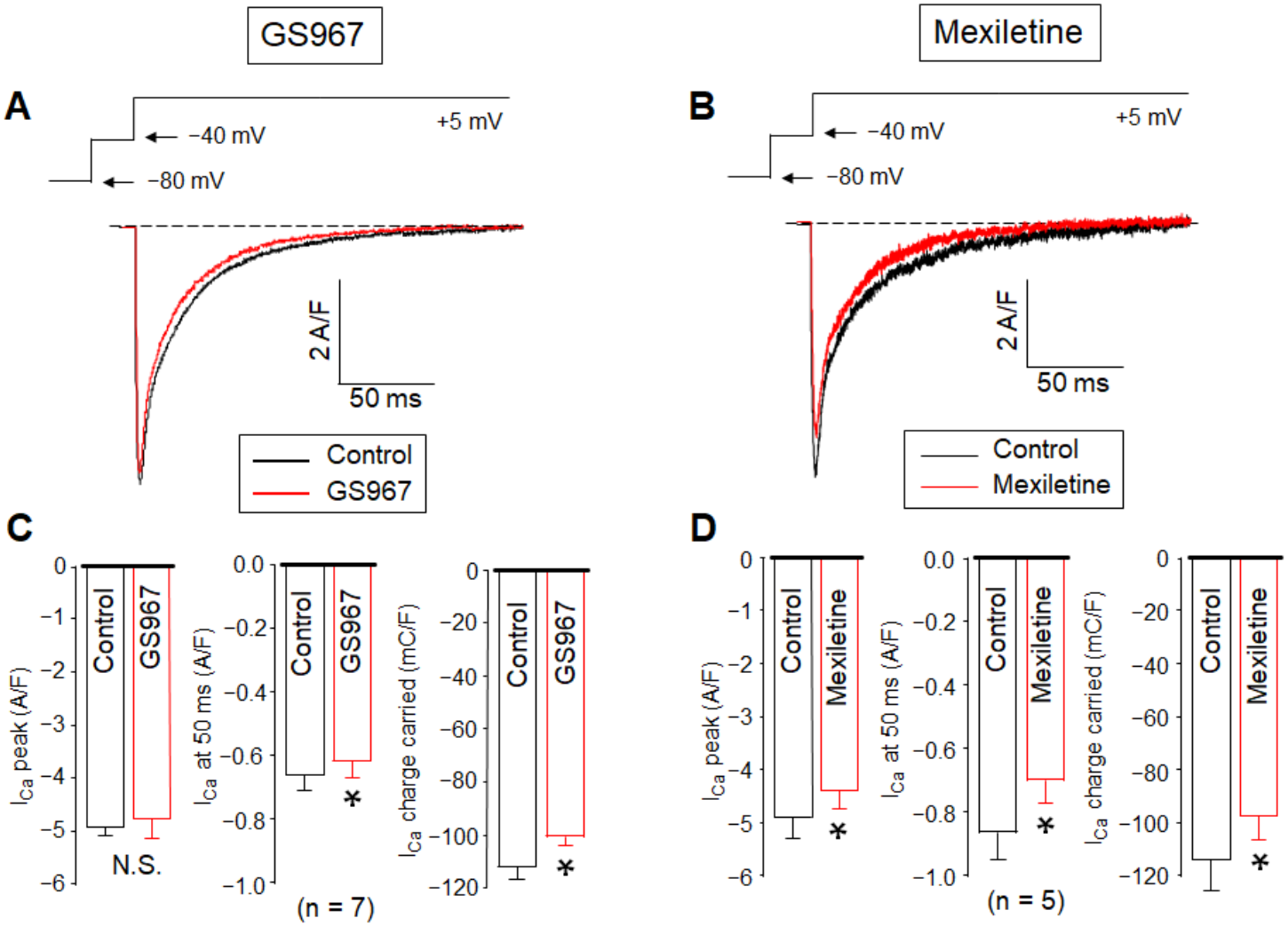

Figure 4

Effects of 1 μM GS967 (A,C) and 40 μM mexiletine (B,D) on ICa under conventional voltage clamp conditions using test pulses of 200 ms duration clamped to +5 mV from the holding potential of −80 mV following a 15 ms duration prepulse to −40 mV. A,B: Representative superimposed analogue ICa records. C,D: Average ICa densities measured as peak currents or 50 ms after beginning the pulse, and ICa integrals. Columns and bars are mean ± SEM, numbers in parentheses indicate the number of myocytes studied, asterisks denote significant differences between the pre-drug control and the GS967- or mexiletine-treated data.

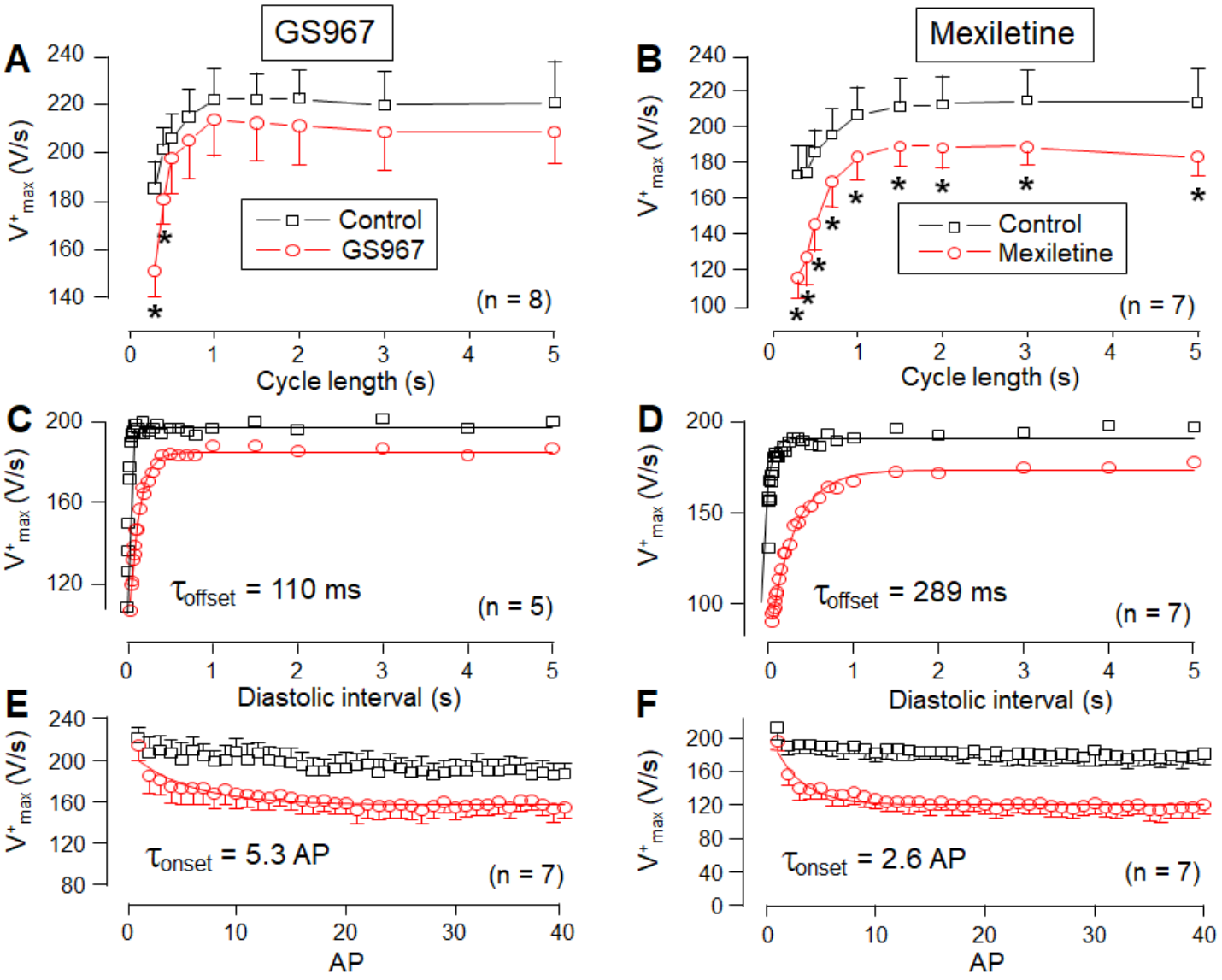

Figure 5

Effects of 1 µM GS967 (A,C,E) and 40 µM mexiletine (B,D,F) on the maximal rate of depolarization (V+max) measured in canine right ventricular trabeculae. A,B: Cycle length-dependent effects on V+max under steady-state conditions. C,D: Determination of offset kinetics of GS967 and mexiletine as indicated by the time-dependent restitution of V+max. E,F: Determination of the onset kinetics of the V+max-block at 2.5 Hz. See the experimental details in the Methods section. Solid lines were obtained by monoexponential fitting. Symbols and bars are mean ± SEM, numbers in parentheses indicate the number of myocytes studied, asterisks denote significant differences between the pre-drug control and the GS967- or mexiletine-treated data.

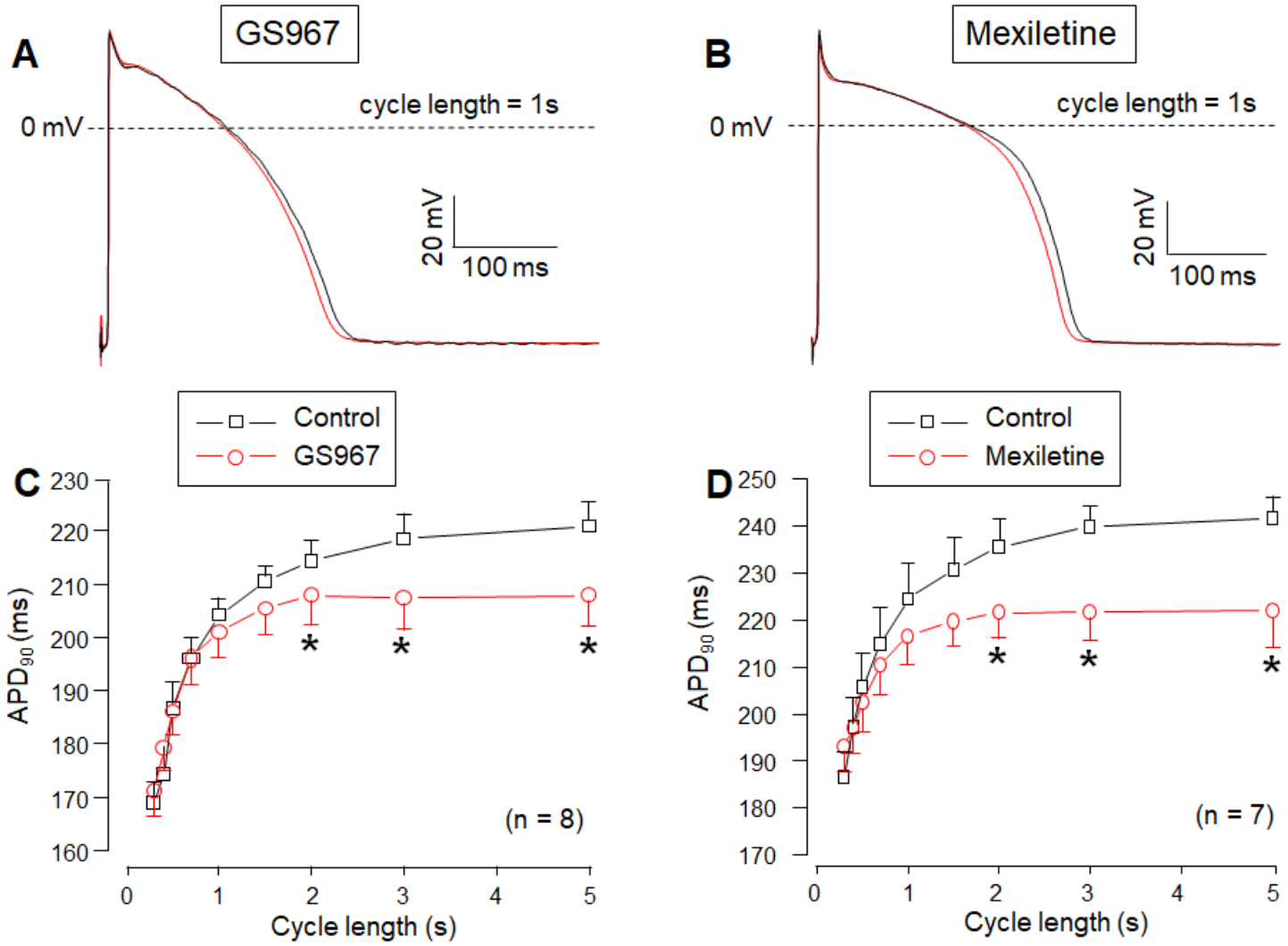

Figure 6

Cycle length-dependent effects of GS967 (A,C) and mexiletine (B,D) on AP duration measured at 90% of repolarization (APD90) in canine right ventricular trabeculae under steady-state conditions. During the experiments the cycle length was gradually changed between 0.3 and 5 s. A,B: Representative superimposed analogue action potential pairs obtained at the constant pacing cycle length of 1 s before and after superfusion with 1 μM GS967 or 40 μM mexiletine. C,D: Average rate-dependent APD values. Symbols and bars are mean ± SEM, numbers in parentheses indicate the number of myocytes studied, asterisks denote significant differences between the pre-drug control and the GS967- or mexiletine-treated data.

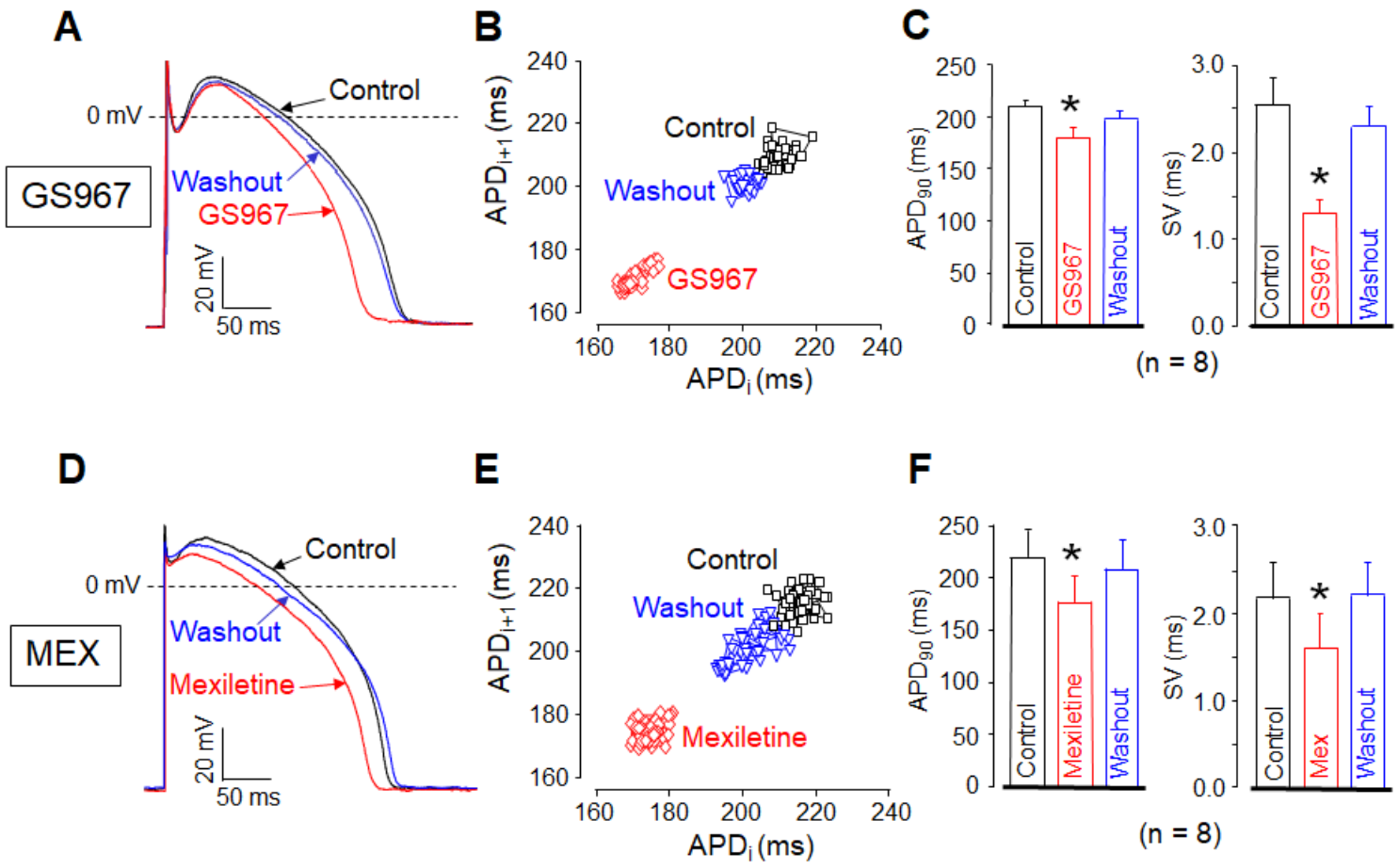

Figure 7

Reversible effects of GS967 (A-C) and mexiletine (D-F) on beat-to-beat variability of APD in isolated myocytes. Superimposed sets of action potentials (A,D) and Poincaré plots (B,E) obtained in control, after exposure to 1 μM GS967 or 40 μM mexiletine, and after washout of drugs. Panels C and F show the average effects on beat-to-beat variability (SV) and APD. Columns and bars are mean ± SEM, numbers in parentheses indicate the number of myocytes studied, asterisks denote significant differences between the pre-drug control and the GS967- or mexiletine-treated data.